D.A Dolmatov, Associated professor
Masoud Hajivand, PhD student
National Aerospace University named after N. E Zhukovsky «Kharkiv Aviation Institute »

RANS SIMULATION OF EFFECT OF AIR ADMISSION'S HOLES GEOMETRY IN A GAS TURBINE COMBUSTOR AND THEIR EFFECTS ON EMISSION CARACTERISTTCS

This study was carried out to investigate the effects of geometry and location of different air admission holes (secondary, dilution) on total temperature characteristics and formation of nitrogen oxide emissions in a can combustor flame tube, for 8 various cases, using computational fluid dynamics (CFD) .The simulation has been performed using ANSYS CFX including laminar flamelet model, for simulation of non premixed methane-air combustion and thermal and prompt nitrogen oxide (NOx) formation was performed to predicting NOx emission characteristics with a K-epsilon model of turbulent.

Key words: air admission holes, emission, combustion, CFD, nitrogen oxide,combustor

Introduction. Nowadays, the optimization of combustion performance and the reduction of pollutant emissions require considerable research efforts from the gas turbine industry. The basic objectives in combustor design are to achieve easy ignition, high combustion efficiency and minimum pollutant emissions [1]. Environmental regulations on gas turbine, including NOx emissions, have been enhanced over the past several years. Therefore, technologies for accurately predicting the amount of NOx emission from the combustor, the emission source of the gas turbine engine, are very important [2].

Due to increasing global environmental awareness, the control of gas turbine emissions, targeting those in small quantities such as NOx, CO, has become more stringent. The combustor, which is one of the core components of an gas turbine engine and a source of such emissions, will increasingly become the focus of future engine development. Development of combustors for gas turbine engines typically takes considerable time and incurs large costs, because such development includes the process of fabricating an extensive amount of combustor hardware that complies with the required specifications using existing products and data, as well as the process of satisfying the performance specifications through trial and error, mainly through repeated experiments and design improvements. Therefore, if these processes can be substituted with numerical prediction, the time period and the cost of combustor development can be reduced considerably. However, because the internal flow of an gas turbine engine combustor consists of complicated phenomena, including turbulent mixing along with spraying, atomizing, and swirling of liquid and gas fuel, as well as a huge number of chemical reaction mechanisms, reproduction through numerical simulation is very difficult, and even today there are few tools with sufficiently high prediction accuracy for this purpose. In recent years, Large Eddy Simulation (LES), which has a small number of adjustment parameters for modeling and can simulate unsteady turbulent flow, has attracted a great deal of attention. However, LES has not been established as a practical design tool for actual combustors, because the atomization model and turbulence combustion model for the spray combustion field of LES are still in the study phase and the calculation load of LES is very high; therefore, significant computer resources are required. Accordingly, the main method used in current study is Reynolds-Averaged Navier-Strokes (RANS) simulation, which obtains a steady mean field where turbulence phenomena are averaged. RANS simulation has lower accuracy than LES, but it can be used sufficiently as a design tool through proper interpretation of its results due to its reasonable computational costs.[2]

The gas turbine can-combustor is designed to burn the fuel efficiently, reduce the emissions, and lower the wall temperature. In this study various geometrical parameters of air admission holes on the combustor liner, and position of dilution holes are changed to investigate the effect of these parameters on combustion chamber performance and emissions. In this study the mathematical models used for combustion consist of the PDF flamelet model for non-premixed methane-air combustion. The outcome of the work will help in finding out the geometry of the circular air supply on the combustion chamber liner, which will lead to less emission.

The flow visualization technique was demonstrated by Koutmos and McGuirk [3] in can-combustor model. They experimented a benchmark study on the investigation of the three-dimensional flow field water model. Flow visualization demonstrated that internal flow patterns simulated closely those expected in real combustors. The combustor comprised a swirl driven primary zone, annulus fed primary and dilution jets and an exit contraction nozzle. LDA measurements of the three mean velocity components and corresponding turbulence intensities were obtained to map out the flow development throughout the combustor. Besides providing information to aid understanding of the complex flow events inside combustors, the data are believed to be of sufficient quantity and quality to act as a benchmark test case for the assessment of the predictive accuracy of computational models for gas-turbine combustors. Aside from the flow visualization study, Eldrainy et al. [4] examined the flow inside the

combustor. The flow field inside the combustor is controlled by the liner shape and size, wall side holes shape, size and arrangement (primary, secondary, and dilution holes), and primary air swirler configuration. Air swirler adds sufficient swirling to the inlet flow to generate central recirculation region which is necessary for flame stability and fuel air mixing enhancement. Therefore designing an appropriate air swirler is a challenge to produce stable, efficient and low emission combustion with low pressure losses. The flow behavior was investigated numerically using CFD solver. This study has provided physical insight into the flow pattern inside the combustion chamber. The necessity of the problem is to evaluate the NOx emission after the combustion process. There are strict regulations on aircraft emissions of pollutants like CO and NOx, so combustors need to be designed to minimize those emissions. In this work, an examination about the emission of unburned gases is predicted by motility the air holes in the secondary chamber. The main objective of this study is to diminish the NOx emission and to establish the effective location and size of secondary and dilution holes for cooling the combustion products.

In present study an attempt has been made through CFD approach to analyze the flow pattern with in combustion and through air admission holes and from these the temperature and NO distribution in the chamber as well as the temperature and NO quality at the exit of combustion chamber is obtained.

Combustor zones .a conventional combustor comprises of three basic zones - primary, intermediate and dilution.

Primary zone. The main function of the primary zone is to anchor the flame and provide sufficient time, temperature, and turbulence to achieve essentially complete combustion of the incoming fuel–air mixture. The importance of the primary-zone airflow pattern to the attainment of these goals cannot be overstated. Many different types of flow patterns are employed, but one feature that is common to all is the creation of a toroidal flow reversal that entrains and recirculates a portion of the hot combustion gases to provide continuous ignition to the incoming air and fuel. Some early combustors used air swirlers to create the toroidal flow pattern, whereas others had no swirler and relied solely on air injected through holes drilled in the liner wall at the upstream end of the liner . An important contribution to primary-zone aerodynamics was made by the Lucas combustion group in their combustor designs for the Whittle W2B and Welland engines. The basic airflow patterns embodied in the Lucas concept are sketched in Figure 1 . Note that both swirling air and primary air jets are used to produce the desired flow reversal. As already noted, each mode of air injection is capable of achieving flow recirculation in its own right, but if both are used, and if a proper choice is made of swirl vane angle and the size, number, and axial location of the primary air holes, then the two separate flow recirculations created by the two separate modes of air injection will merge and blend in such a manner that each one complements and strengthens the other. The result is a strong and stable primary-zone airflow pattern that can provide wide stability limits, good ignition performance, and freedom from the type of flow instabilities that often give rise to combustion pulsations and noise. The Lucas company had a strong influence on British combustor design, and the basic aerodynamic features shown in Figure 1 can be found in the combustors designed for many British engines, including the Rolls Royce Nene, Derwent, Dart, Proteus, Avon, Conway, and Tyne. [5]

Intermediate zone. If the primary-zone temperature is higher than around 2000 K, dissociation reactions will result in the appearance of significant concentrations of carbon monoxide (CO) and hydrogen (H2) in the efflux gases. Should these gases pass directly to the dilution zone and be rapidly cooled by the addition of massive amounts of air, the gas composition would be “frozen,” and CO, which is both a pollutant and a source of combustion inefficiency, would be discharged from the combustor unburned. Dropping the temperature to an intermediate level by the addition of small amounts of air encourages the burnout of soot and allows the combustion of CO and any other unburned hydrocarbons (UHC) to proceed to completion. In early combustor designs, an intermediate zone was provided as a matter of course. As pressure ratios increased, and more air was required for combustion and liner-wall cooling, the amount of air available for the intermediate zone went down accordingly. By around 1970, the traditional form of intermediate zone had largely disappeared. However, the desirability of an intermediate zone remains; therefore, should the developments now being made in wall-cooling techniques allow some air to become available, consideration might be given to its possible reinstatement [5].(see Fig 2)

Dilution zones. The role of the dilution zone is to admit the air remaining after the combustion and wall cooling requirements have been met, and to provide an outlet stream with a temperature distribution that is acceptable to the turbine. This temperature distribution is usually described in terms of “pattern factor” or “temperature traverse quality.” The amount of air available for dilution is usually between 20 and 40% of the total combustor airflow. It is introduced into the hot gas stream through one or more rows of holes in the liner walls. The size and shape of these holes are selected to optimize the penetration of the air jets and their subsequent mixing with the main stream. In theory, any given traverse quality can be achieved either by the use of a long dilution zone or by tolerating a high liner pressure-loss factor. In practice, however, it is found that mixedness initially improves greatly with an increase in mixing length and thereafter at a progressively slower rate. This is why the length/diameter ratios of dilution zones all tend to lie in a narrow range between 1.5 and 1.8. For the very high turbine entry temperature (around 2000 K) associated with modern high-performance engines, an ideal pattern factor would be one that gives minimum temperature at the turbine blade root, where stresses are highest, and also

at the turbine blade tip, to protect seal materials. Attainment of the desired temperature profile is paramount, owing to its major impact on the maximum allowable mean turbine entry temperature and hot-section durability. Due to the importance and severity of the problem, a large proportion of the total combustor development effort is devoted to achieving the desired pattern factor. The locations of the three main zones described above, in relation to the various combustor components and the air admission holes, are shown in Figure 2. Note also in this figure the "snout," which is formed by cowls that project upstream from the dome. The region inside the snout acts as a plenum chamber, providing a high uniform static pressure for feeding the air swirler, which is attached to the dome, the airblast atomizer, and the dome cooling airflows [5] .

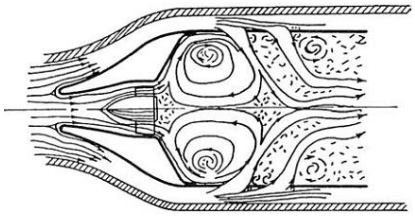

Fig1. Lucas primary-zone airflow pattern.

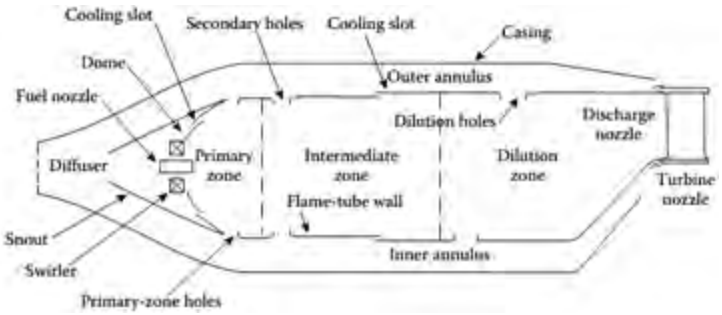

Fig2. Lucas Main components of a conventional combustor.

Governing equations and turbulence and combustion model. The mathematical equations describing the fuel combustion are based on the equations of conservation of mass, momentum, and energy together with other supplementary equations for the turbulence and combustion. The standard k-ε turbulence model is used in this paper. The equations for the turbulent kinetic energy k and the dissipation rate of the turbulent kinetic energy ε are solved Several models of turbulence have been put forward by different authors. These models differ in complexity and range of applicability; they also involve the solution of different numbers of differential equations. The turbulence model incorporated in this work is the high Reynolds number k-ε two equation model. This model requires the solution of two differential equations, for the two turbulence properties: the kinetic energy of turbulence k, and its dissipation rate ε. The model is moderate in complexity. It has been extensively used by many investigations and has proved to be adequate over a wide range of flow situation. Here the governing differential equations are presented below in details (Launder, and Spalding, 1974).

Differential equations for turbulence-energy k and dissipation rate ε used in combustion are respectively as follows:

$$\frac{\partial(\rho k)}{\partial t} + \nabla \cdot (\rho U k) = \nabla \cdot \left[\left(\mu + \frac{\mu_t}{\sigma_g}\right)\nabla k\right] + P_k - \rho\varepsilon \quad (1)$$

$$\frac{\partial(\rho \varepsilon)}{\partial t} + \nabla \cdot (\rho U \varepsilon) = \nabla \cdot \left[\left(\mu + \frac{\mu_t}{\sigma_g}\right)\nabla \varepsilon\right] + \frac{\varepsilon}{k}(C_{\varepsilon 1} P_k - C_{\varepsilon 2}\rho\varepsilon) \quad (2)$$

For non premixed combustion modeling. All the numerical simulation has been performed using the Computational Fluid Dynamics (CFD) commercial code ANSYS CFX release 16, including laminar flamelet model for modeling non-premixed methane-air combustion with 17 spices and 55 reactions.

In the flamelet model chemical reaction rates are computed first (independent of the flow) and the relevant scalar properties are stored in lookup tables accessible by the flow solver. The instantaneous scalar properties φ (i.e., temperature, density, compositions) are represented as a function of the instantaneous mixture fraction Z and its variance $Z''2$, and the scalar dissipation χ : $\varphi = \varphi(Z, Z''2, \chi)$. Mean scalar properties are then computed by integrating the instantaneous φ over an assumed β-PDF, and the results are stored in the lookup tables. In the flamelet approach, transport equations for the turbulent kinetic energy (k), its dissipation rate (ε), enthalpy, mixture fraction Z, and its variance $Z''2$ (which is used to compute the scalar dissipation) are solved for each computationalcell. These values are then used to extract mean scalar properties from the chemistry lookup tables. The flow field properties are updated and iterations continue until convergence criteria are met. The *NO* x formation model (based on thermal and prompt mechanisms) is also included.

When modeling NO*x* formation in methane-air combustion, the thermal NO and prompt NO are taken into account. In the simulation process, we solve the mass transport equation for the NO species, taking into account convection, diffusion, production and consumption of NO and related species. This approach is completely general, being derived from the fundamental principle of mass conservation. For thermal and prompt NO*x* mechanisms, only the following NO species transport equation is needed:[6]

$$\rho\frac{\partial Y_{NO}}{\partial t}+\rho u_i\frac{\partial Y_{NO}}{\partial x_i}=\frac{\partial}{\partial x_i}\left(\rho D\frac{\partial Y_{NO}}{\partial x_i}\right)+S_{NO} \quad (3)$$

The source term S_{NO} is to be determined for different NOx mechanism. YNO is mass fraction of NO species in the gas phase and D is effective diffusion coefficient.

Geometry of combustor ,meshing and boundary condition. The domain of simulation, is a can type of combustor. The geometrical sizes of the combustor, fuel injector , air swirler and the fuel inlet (methane) and oxidizer inlet (air) and all of the geometrical sizes of combustor are shown in fig.3 without any secondary or intermediate and dilution holes on flame tube (liner). Methane and air are entered in the domain separately. The model was meshed for simulating in a tetrahedrons meshing method, with about total number of 2016000 nodes, and 7 600 000 total number of elements including prismatic layers around the walls of combustor .The different boundary conditions applied for flow analysis of gas turbine can-type combustion chamber in this investigation, which they are inlet mass flow rate for both fuel and oxidizer entering the domain , outlet average static press ure and with no slip walls. Boundary condition information are shown in table1.

Fig3. Can-combustor 1-air inlet(diffuser) 2-axial swirler 3-casing 4-flametube(liner) 5-methan injector

Table1.

boundary condition information of combustor

Operating pressure (atm)	4
Temperature entering in combustor [K]	450
oxidizer mass flow rate [kg/s]	0.3
Temperature of fuel (K)	310
Fuel mass flow rate [kg/s]	0.004

Cases of study. in this study 8 cases of combustor with different geometrical parameters and location of primary and dilution holes were studied .The form of holes admissions are circular on flametube (liner) of combustor. The general form of air admission holes are shown in figure.4 on the combustor flame tube for 8 various cases. Each cases comprises its own air admission zones and their geometrical parameters and location. A zone is primary zone of air admission and B zone is secondary zone. Some cases comprises 2 zones for primary and 2 zone for secondary air admissions like cas-5 and case 2.

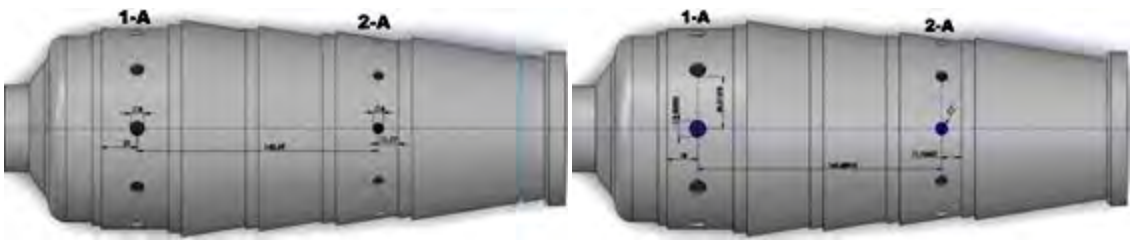

a) b)

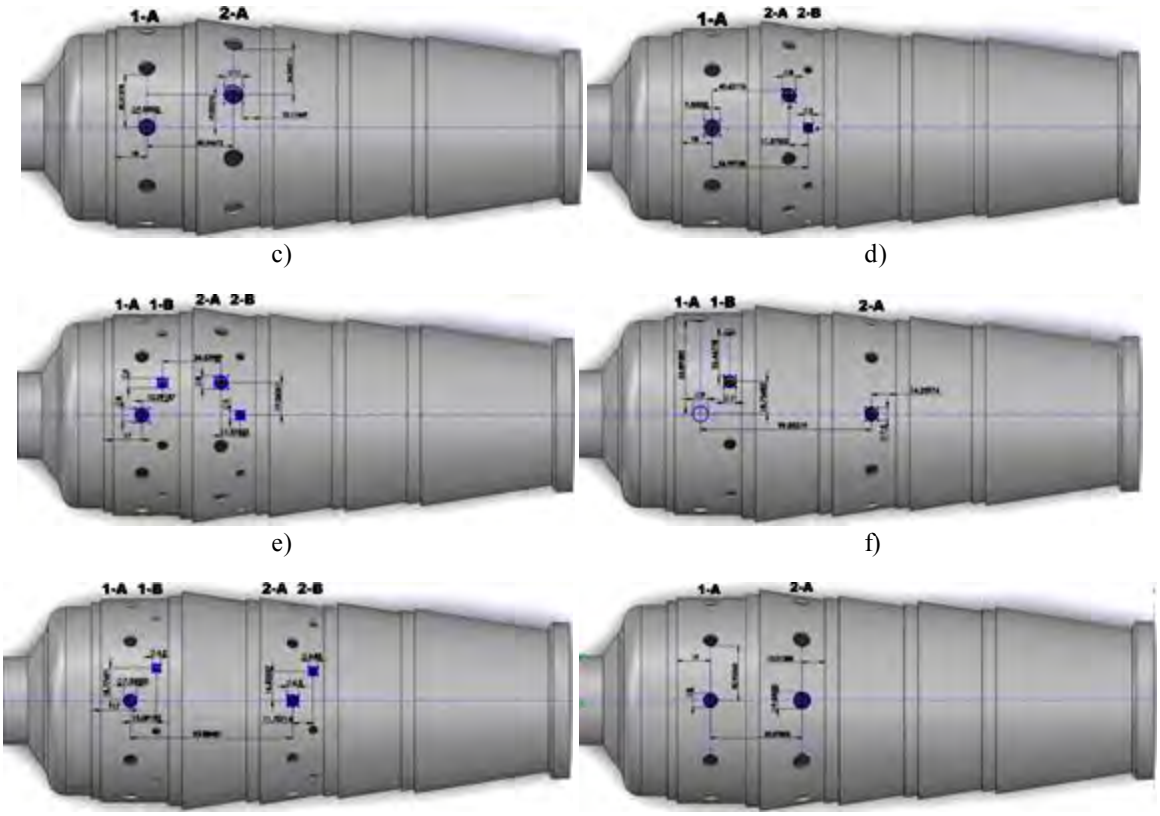

c) d)

e) f)

g) h)

Fig4. Can-combustors with various geometry and location of air admission holes a)case-1, b)case-2, c)case-3, d)case-4, e)case-5, f)case-6, g)case-7, h)case-8

The table of information of geometry and location of air admission holes. All of the information about the studied cases and detailed geometrical parameters of air admission holes of combustors are shown in table 2-3-4.Table 4 shows the axial distances each air admission holes to another zones.

Table2.

Geometrical parameters and locations of air admission holes for cases1-4

cases	**1**		**2**		**3**		**4**		
zones	1-A	1-B	1-A	1-B	1-A	1-B	1-A	2-A	2-B
diameter (mm)	8	6	9.5	7	9.5	11	9.5	8	5
amount	10	10	10	10	10	10	10	10	10
location	parallel		parallel		Zig-zag		-	Zig-zag	
form	circular		circular		circular		circular		

Table3.

Geometrical parameters and locations of air admission holes for cases5-8

cases	**5**				**6**			**7**				**8**	
zones	1-A	1-B	2-A	2-B	1-A	1-B	2-A	1-A	1-B	2-A	2-B	1-A	2-A
Diametr (mm)	8	6	8	5	9	7	7.5	7.5	4.5	6.5	4.85	8	9.5
amount	10	10	10	10	5	10	10	10	10	10	10	10	10
location	Zigzag		Zigzag		Zigzag		-	Zigzag		Zigzag		parallel	
form	circular				circular			circular				circular	

Table4.

axial distances of air admission holes from the center of circular holes from zone to another zones

cases	**1**	**2**	**3**	**4**	**5**	**6**	**7**	**8**
1-A to 2-A (mm)	140.69	143.69	50.54	45.62	46.62	17.1	93.88	52.1
1-A to 2-B (mm)	-	-	-	57	58	99.83	105.58	-
1-A to 1-B (mm)	-	-	-	-	12.1	82.73	15.1	-
1-B to 2-A (mm)	-	-	-	-	34.52	-	78.78	-
1-B to 2-B (mm)	-	-	-	-	45.9	-	90.48	-
2-A to 2-B (mm)	-	-	-	-	11.37	-	11.7	-

Results and discussion of simulation-(Total temperature and NO distribution in the 8 various cases). All of 8 cases of simulation was performed in ANSYS CFX [7]. The convergence criteria in this simulation was at the RMS residual type with the 10^{-4} residual target and automatic time scale control and time scale factor of 1 .All the simulation in 8 cases were converged successfully with solving the mass and momentum (U, V, W momentums), heat transfer (energy), turbulence (k-ε), mass fraction of NO, mixture fraction including mean and variance, temperature variance for predicting NO.

The high value of mass fraction of NO formed indicates an efficient combustion process. In all 8 cases he peak gas temperature is located in the primary zone where combustion of mixture air and methane takes place. The fuel from injector is first mixed in the swirling air before burning in the primary reaction zone. The gas temperature decreases after the primary zone. In case there will be dilution holes are provided at dilution zone, to reduce the temperature this can be done when the temperature inside the combustor is high.

The thermodynamic parameter called temperature influences the flow inside the combustion chamber. To prognosticate this parameter, the selection of air admission holes with respect to the location and geometry of them is necessary. Figures 5-12 demonstrates the total temperature and NO distribution for the can-combustor with different zones of air admission holes . The total temperature increases gradually due to the chemical reaction inside the main combustor. In all cases it is clear that after the location of first cooling zone and air admission holes , the temperature diminishes due to the cooling effect of air entering into combustor. Thus, it is distinct to show that the case1 which has 2 zones of air admission holes, then in figure 5a there is 2203[K] of maximum total temperature in the first zone of combustion in combustor liner and the maximum and minimum total temperature is 1142[K] and 946[K] at the outlet area of combustor which has shown in figure 13a and besides that figure 5b shows that this case has the 167 ppm of maximum of NO concentration in whole combustor so the maximum NO concentration at the outlet area of this case is 16.77ppm and the minimum is 7.343ppm which has shown in figure 14a.

The case-2 has 2 zones of air admission holes, then in figure 6a there is 2181[K] of maximum total temperature in the first zone of combustion in combustor liner and the maximum and minimum total temperature is 1222[K] and 920[K] at the outlet area of combustor which has shown in figure 13b and besides that figure 6b shows that this case has the 167 ppm of maximum NO concentration in whole combustor so the maximum NO concentration at the outlet area of this case is 18.86ppm and the minimum is 6.8ppm which has shown in figure 14b.

The case-3 has 2 zones of air admission holes in a zigzag form of location, then in figure 7a there is 2221[K] of maximum total temperature in the first zone of combustion in combustor liner and the maximum and minimum total temperature is 1304[K] and 904[K] at the outlet area of combustor which has shown in figure 13c and besides that figure 7b shows that this case has the 130.8 ppm of maximum NO concentration in whole combustor so the maximum NO concentration at the outlet area of this case is 23.07ppm and the minimum is 4.437ppm which has shown in figure 14c.

The case-4 has 2 zones of air admission holes. The second zone has 2 rows of holes (2A-2B)in a zigzag form of location , then in figure 8a there is 2219[K] of maximum total temperature in the first zone of combustion in combustor liner and the maximum and minimum total temperature is 1253[K] and 965[K] at the outlet area of combustor which has shown in figure 13d and besides that figure 8b shows that this case has the 149.4ppm of maximum NO concentration in whole combustor so the maximum NO concentration at the outlet area of this case is 19.9ppm and the minimum is 5.83ppm which has shown in figure 14d.

The case-4 has 2 zones of air admission holes. The second zone has 2 rows of holes (2A-2B)in a zigzag form, then in figure 8a there is 2219[K] of maximum total temperature in the first zone of combustion in combustor liner and the maximum and minimum total temperature is 1253[K] and 965[K] at the outlet area of combustor which has shown in figure 13d and besides that figure 8b shows that this case has the 149.4ppm of maximum NO concentration in whole combustor so the maximum NO concentration at the outlet area of this case is 19.9ppm and the minimum is 5.83ppm which has shown in figure 14d.

The case-5 has 2 zones of air admission holes. The first and second zone have 2 separate rows of holes (1A-1B)and(2A-2B)in a zigzag location , then in figure 9a there is 2217[K] of maximum total temperature in the first zone of combustion in combustor liner and the maximum and minimum total temperature is 1597[K] and 755[K] at the outlet area of combustor which has shown in figure 13e and besides that figure 9b shows that this case has the 104.4ppm of maximum NO concentration in whole combustor so the maximum NO concentration at the outlet area of this case is 41.78ppm and the minimum is 1.537ppm which has shown in figure 14e.

The case-6 has 2 zones of air admission holes. The second zone (IA-1B)has 2 separate rows of holes in a zigzag location , then in figure 10a there is 2174[K] of maximum total temperature in the first zone of combustion in combustor liner and the maximum and minimum total temperature is 1213[K] and 890[K] at the outlet area of combustor which has shown in figure 13f and besides that figure 10b shows that this case has the 153.5ppm of maximum NO concentration in whole combustor so the maximum NO concentration at the outlet area of this case is 19.1ppm and the minimum is 7.33ppm which has shown in figure 14f.

The case-7 has 2 zones of air admission holes. The first and second zone have 2 separate rows of holes (1A-1B)and(2A-2B)in a zigzag location , then in figure 11a there is 2251[K] of maximum total temperature in the first zone of combustion in combustor liner and the maximum and minimum total temperature is 1415[K] and 849[K] at the outlet area of combustor which has shown in figure 13g and besides that figure 11b shows that this case has the 209.8ppm of maximum NO concentration in whole combustor so the maximum NO concentration at the outlet area of this case is 29.11ppm and the minimum is 5.61ppm which has shown in figure 14g.

The case-8 has 2 zones of air admission holes in a parallel location to each other, then in figure 12a there is 2235[K] of maximum total temperature in the first zone of combustion in combustor liner and the maximum and minimum total temperature is 1242[K] and 949[K] at the outlet area of combustor which has shown in figure 13h and besides that figure 12b shows that this case has the 210.7ppm of maximum NO concentration in whole combustor so the maximum NO concentration at the outlet area of this case is 23.17ppm and the minimum is 8.57ppm which has shown in figure 14h.

In this study the maximum total temperature of 2251[K] with the maximum 210ppm of NO concentration in the primary zone of combustion is for case-7 due to the minimum diameter of holes at first zone which has two rows of holes. This can lead a minimum amount of cooling air in the liner with minimum air penetration through the holes. The general overview of simulation results is presented in table 5.

The outlet parameters in this simulation is most important due to entering to the atmosphere. As we can see from the outlet results in figure-13 and 14,the minimal total temperature and NO concentration can be seen closer to the liner walls of combustor because of the penetration of cooling air into the combustor and the maximum value of them can be seen at the center of outlet area which are showed in figure 13 and 14.The geometry and diameter and location of the air admission holes and amount of air mass flow rate entering to the combustor can lead the flame to the center line of combustor if the diameters and amount of holes are too big this can make the flame instable and can lead the flame to the extinction phenomena.

Pressure loss factor determines the efficiency in combustion. Pressure loss factor should be minimum as possible, there by more pressurized gas will exists it can be determined from inlet and outlet pressures. In the model there is low pressure loss which shows effective pressure in the gas at the exit of the combustor. Beside that the numerical simulation shows that the maximum pressure loss of 2.14% in case-1 due to the 2 zones of air admission holes with minimum of the diameters of the holes and the second zone (1-B) of holes are situated closer to the outlet of combustor but the results has improved that the minimum pressure loss of 1.195 in case-3 due to the maximum diameters of air holes admission with a zigzag location. These 2 zones of holes in case-3 are situated closer to the primary zone of combustion which has the maximum temperature and concentration of NOx. The general overview of simulation results is presented in table 5.

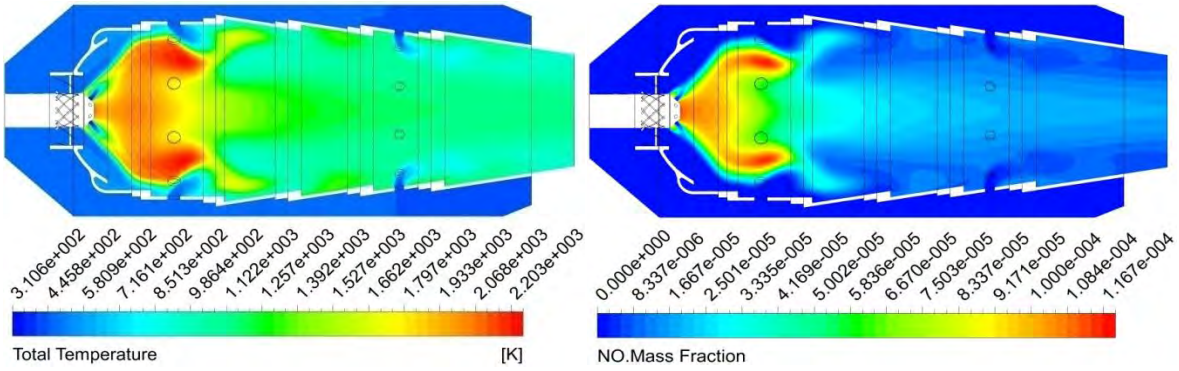

a) b)

Fig 5. Result contours of simulation in case-1- a) Total temperature distribution. b) NO distribution

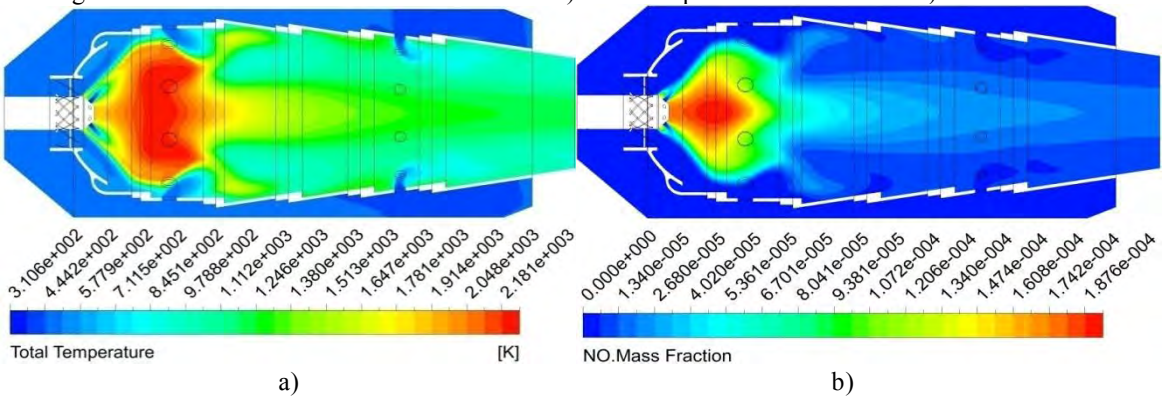

a) b)

Fig 6. Result contours of simulation in case-2 -a) Total temperature distribution. b) NO distribution

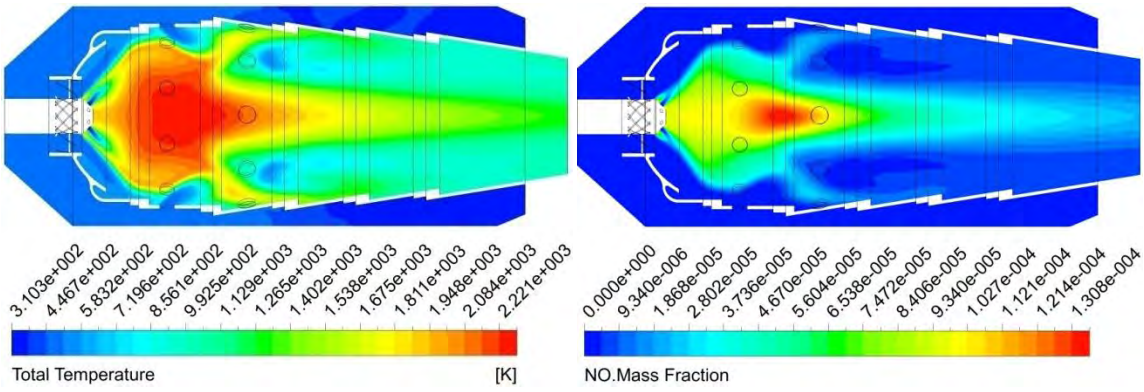

a) b)

Fig 7. Result contours of simulation in case-3- a) Total temperature distribution. b) NO distribution

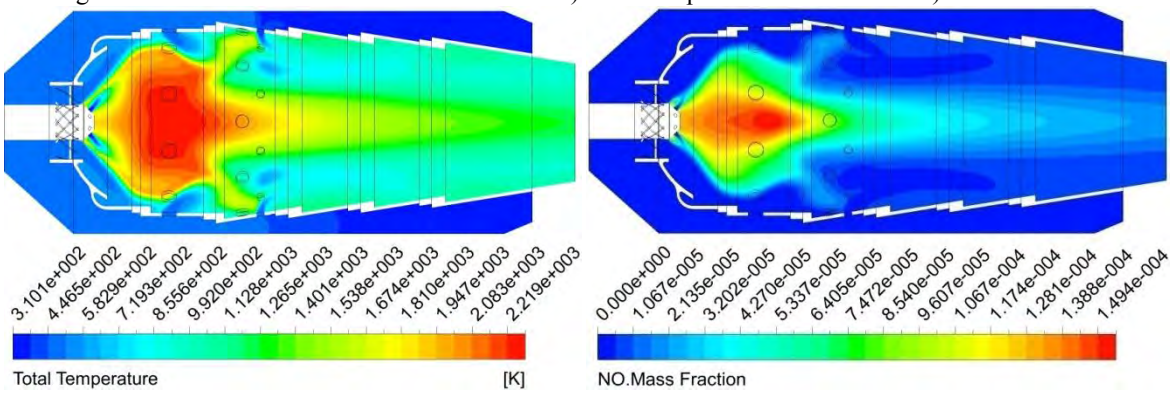

a) b)

Fig 8. Result contours of simulation in case-4- a) Total temperature distribution. b) NO distribution

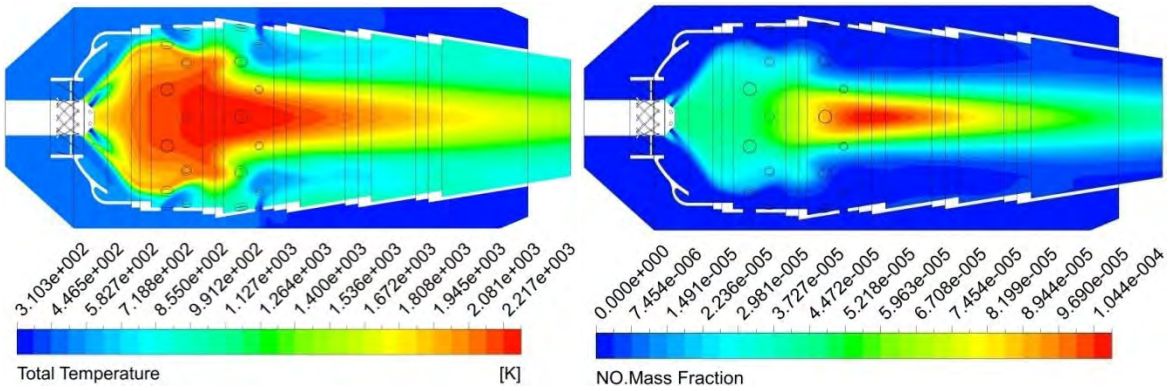

a) b)

Fig 9. Result contours of simulation in case-5- a) Total temperature distribution. b) NO distribution

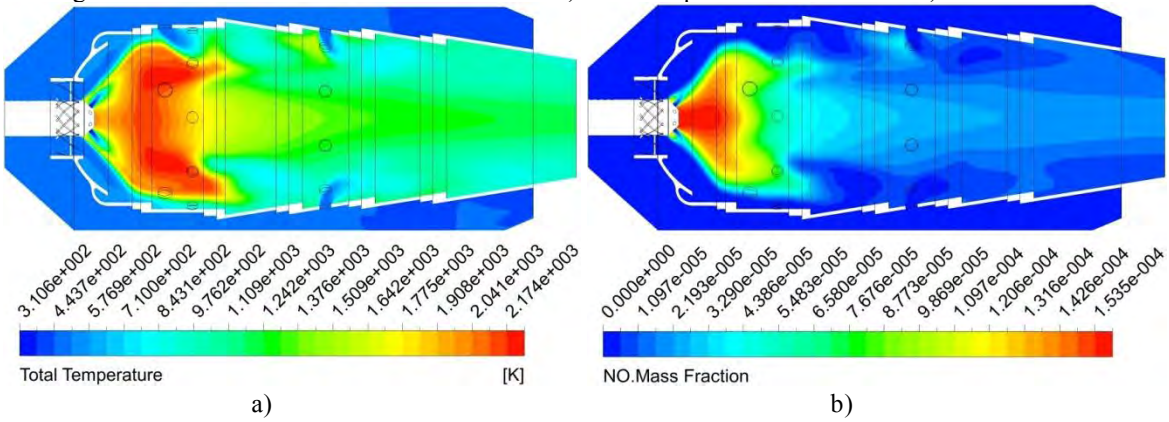

a) b)

Fig 10. Result contours of simulation in case-6- a) Total temperature distribution. b) NO distribution

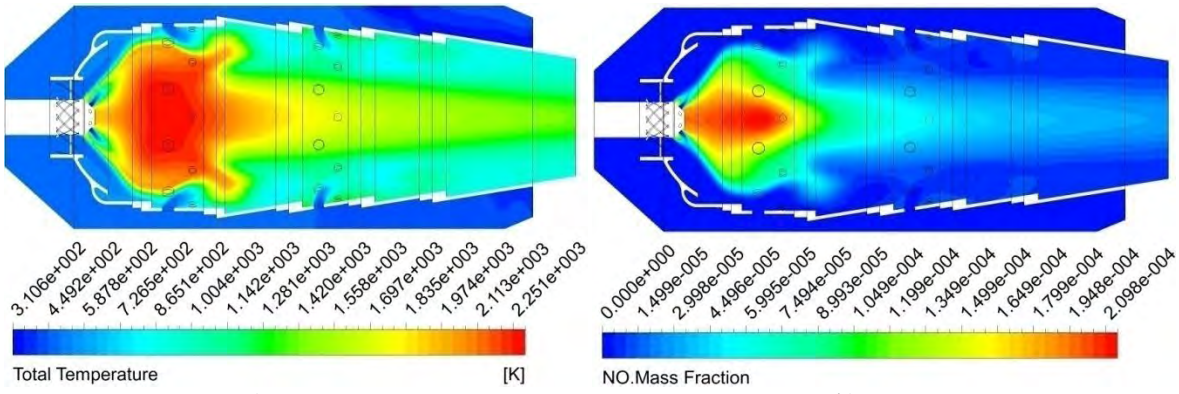

a) b)

Fig 11. Result contours of simulation in case-7- a) Total temperature distribution. b) NO distribution

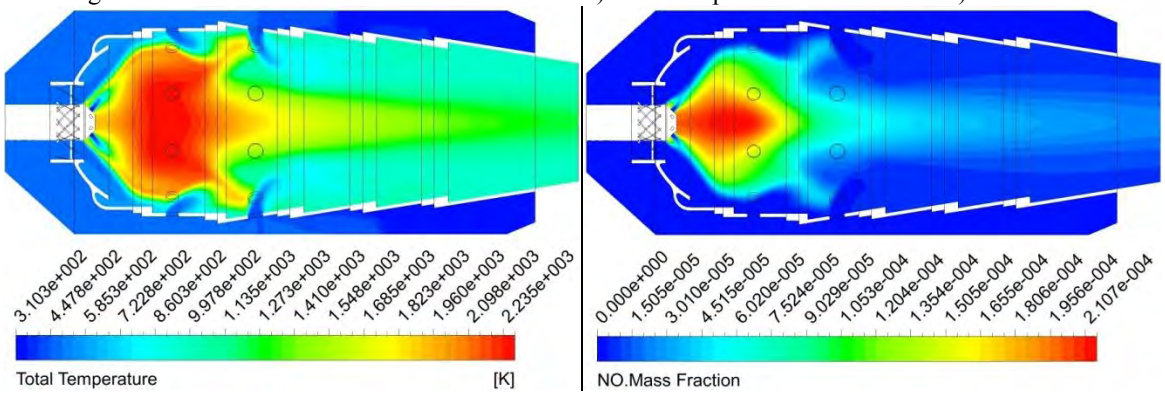

a) b)

Fig 12. Result contours of simulation in case-8- a) Total temperature distribution. b) NO distribution

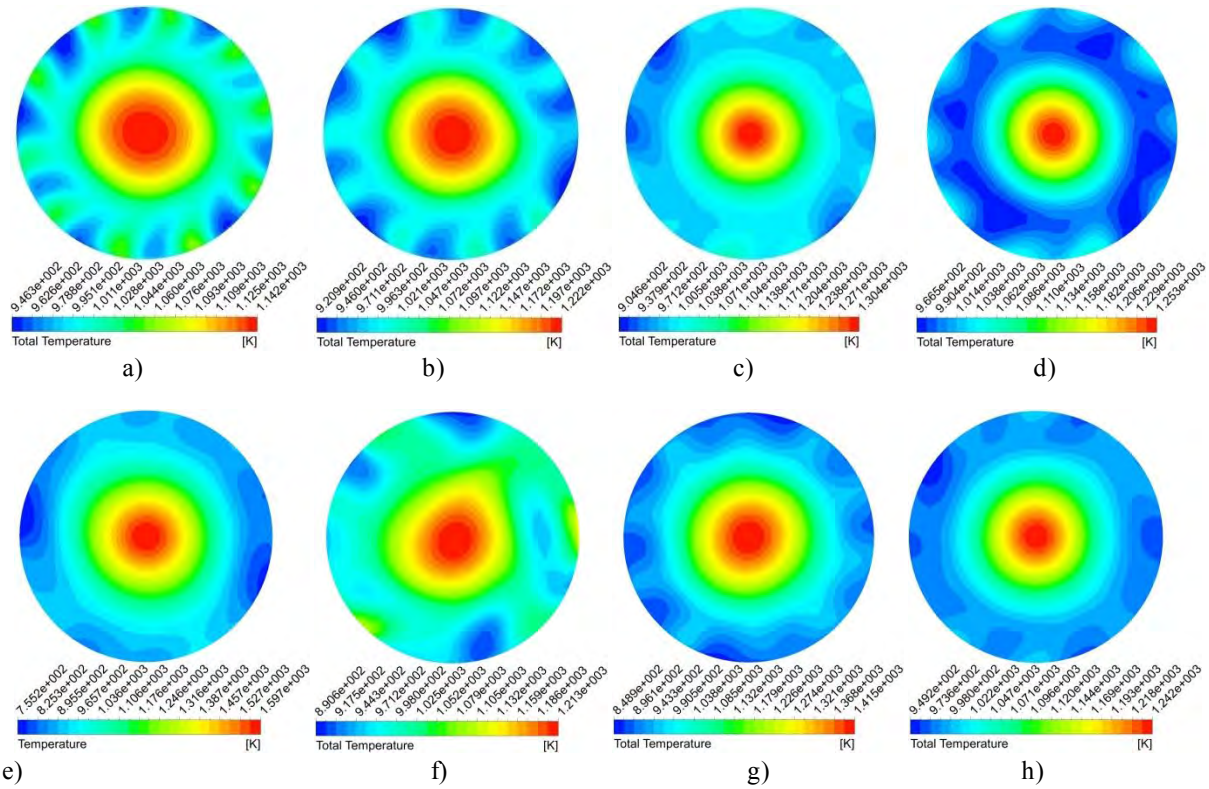

a) b) c) d)

e) f) g) h)

Fig 13. Total temperature distribution at the outlet of combustors for a)case-1, b)case-2, c)case-3, d)case-4, e)case-5, f)case-6, g)case-7, h)case-8

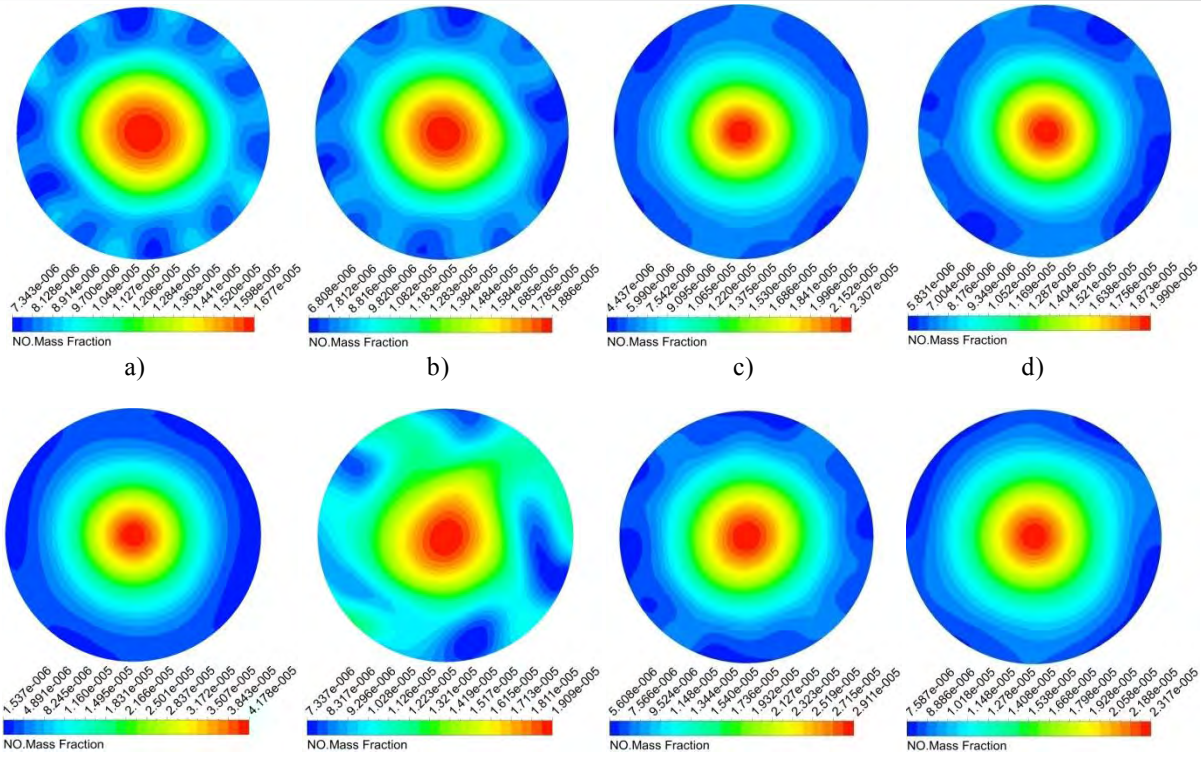

Fig 14. NO concentration distribution at the outlet of combustors for a)case-1, b)case-2, c)case-3, d)case-4, e)case-5, f)case-6, g)case-7, h)case-8

The diagrams of the results-a general overview of simulation results (total temperature and NO concentration)along the centerline of combustors at axial distance are presented in figure 15.

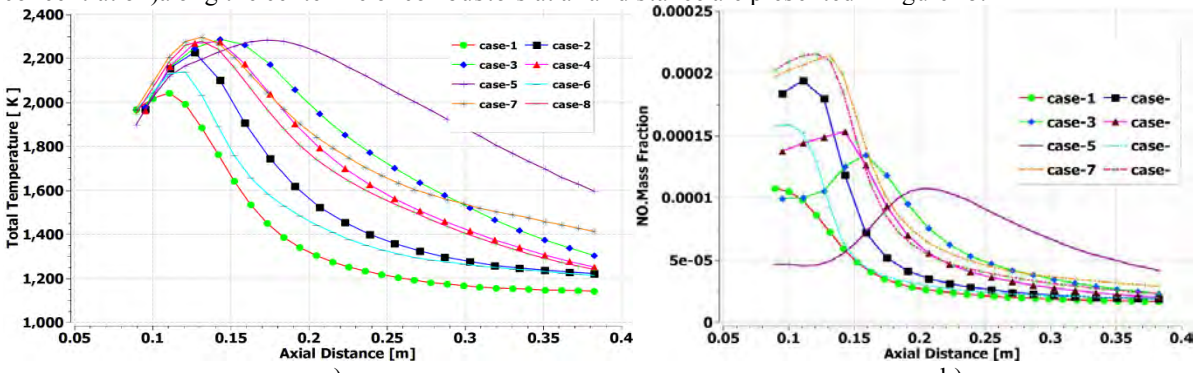

Fig 15. a)Total temperature distribution along the X plane (center line)of combustor b)NO mass fraction distribution along the X plane (center line) of combustor

Table 5.

Numerical results of maximum total temperature and NO distribution and pressure loss in 8 various combustors

Casese	Maximum NO (ppm) in combustor	Maximum Total Temperature [K] in combustor	Pressure loss %
Case-1	167	2203	2.14
Case-2	187.6	2181	1.635
Case-3	130.8	2221	1.195
Case-4	149.4	2219	1.347
Case-5	104.4	2217	1.295
Case-6	153.5	2174	1.597
Case-7	209.8	2251	1.613
Case-8	210.7	2235	1.536

Flow streamline and path along the combustor-In figure 16 we can see the flow path or trajectory along the combustor including the penetration streamlines through the combustor air hole admissions with different geometry of the holes in 8 cases of simulation.

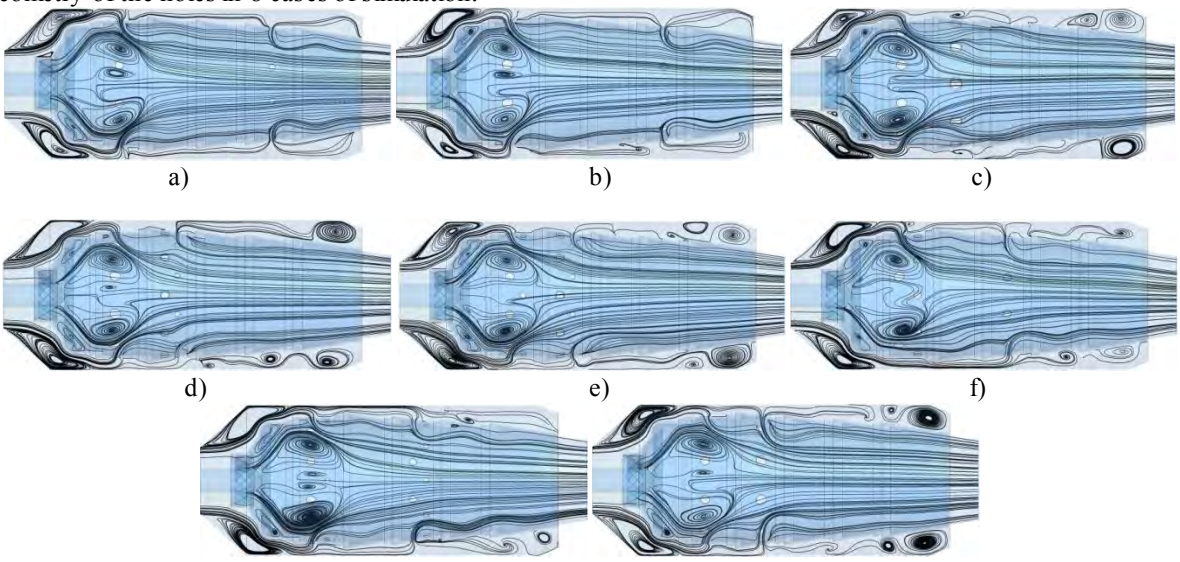

a) b) c)

d) e) f)

g) h)

Fig.16.flow streamline of central recirculation region (CRZ) and flow penetration through the air admission holes into combustor liner along the XY plane of combustor in different cases: a)case-1 b)case-2 c)case-3 d)case-4 e)case-5 f)case-6 g)case-7 h)case-8

Velocity distribution along the combustor-The result of numerical 3-D simulation show that the velocity distribution in 8 cases of combustor depend on various geometry and location of air admission holes and their flow penetration through the holes which are shown in figure 17 for various cases.

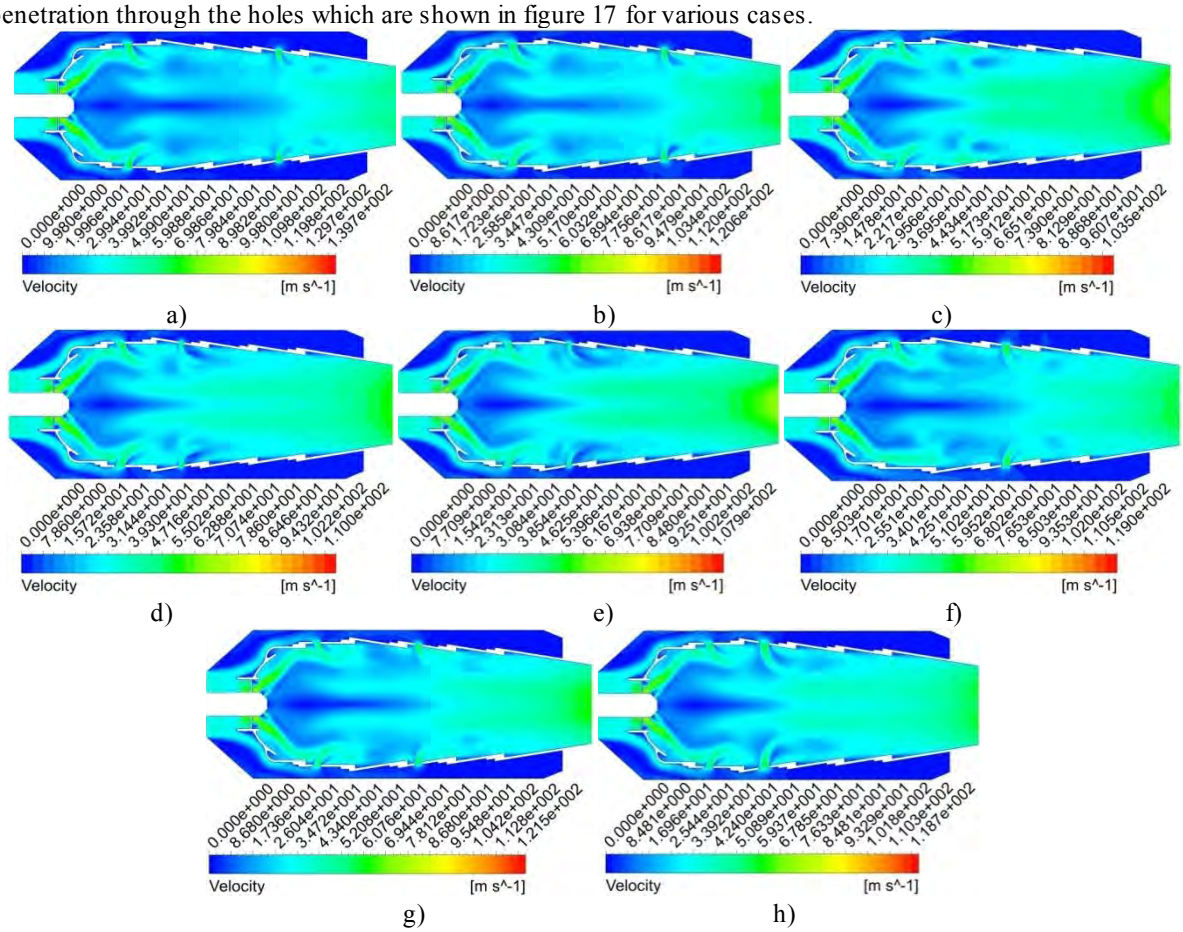

a) b) c)

d) e) f)

g) h)

Fig.17.flow velocity distribution a)case-1 b)case-2 c)case-3 d)case-4 e)case-5 f)case-6 g)case-7 h)case-8

Conclusion- In this study, the effects of the air admission holes geometry and their location in a gas turbine can-combustor liner on NOx performance and temperature distribution were predicted using RANS simulation of computational fluid dynamics (CFD), including ANSYS CFX, for 8 various cases. The results indicated that the use of CFD allows qualitative prediction of the flow inside the combustor and NOx performance and total temperature in it. In all various cases the form and the structure of the flame were significant due to the penetration of air entering through the various air admission holes and their geometrical parameters and the location on the liner of combustor.

The results of this simulation showed that the instability of combustion and the minimum and the maximu m rate of total temperature and formation of NOx has extremely depend on the right designing of air hole admissions it means their geometrical parameters and the location of them in a zigzag form or parallel, closer to the primary zone of combustion or closer to the dilution zone. As the results showed in this simulation every case of study has own properties such as outlet total temperature and NO concentration.

Significant topics of the research was the demonstration of the usefulness of advanced optimization techniques in combustor design and the preliminary validation of the combustion-emission model, a flamelet model of combustion, completed with the thermal and prompt *NOx* formation mechanism. Optimization still requires the use of considerably simplified models and a subsequent refinement phase based on the designer experience, but notwithstanding this is able to improve the design process effectiveness.

References

1. S. R. Razavi S. Tabejamaat.Numerical Simulation of Methane/Air Combustion with CO2 Dilution in A Gas Turbine Combustor. The 5th Fuel & Combustion Conference of Iran Iran University of Science and Technology- Feb. 2014 Amirkabir University of Technology, Tehran, Iran

2. HIDEKI. M. Effects of Dilution Flow Balance and Double-wall Liner on NOx Emission n Aircraft Gas Turbine Engine Combustors . Mitsubishi Heavy Industries Technical Review Vol. 51 No. 4 (December 2014) p.9-15

3. P. Koutmos and J. J. McGuirk, “Isothermal flow in a gas turbine combustor–a benchmark experimental study,” Experiments in Fluids, Vol. 7, 1989, pp. 344-354.

4. Y. A. Eldrainy, J. Jeffrie, and M. Jaafar, “Prediction of the flow inside a Micro Gas Turbine Combustor,” Journal of Mechanical, vol. 25, 2008, pp. 50-63.

5. Arthur H. Lefebvre , Dillip R. Ballal . Gas turbine combustion alternative fuel and emissions /third edition CRC press Taylor and Francis group ,2010.p.560

6. JIANG Bin, Study on NOx Formation in CH4/Air Jet Combustion [Text] / LIANG Hongying ,HUANG Guoqiang,and LI Xingang ,Chinese J. Chem. Eng., vol 14(6)-2006-p.723—728

7. ANSYS CFX-Solver Theory Guide. ANSYS CFX Release 16.0 [Электронный ресурс] / ANSYS, Inc. // Southpointe 275 Technology Drive. – Canonsburg : PA 15317, 2015. – 352 p. – 1 CD-ROM.

УДК 629-735

Д.А Долматов, канд. техн. наук, доцент
Масуд Хаджіванд, Аспирант
Національний аерокосмічний університет ім. М. Є. Жуковського «ХАІ»

RANS МОДЕЛЮВАННЯ ГЕОМЕТРІЇ ВІКОН ПІДВЕДЕННЯ ПОВІТРЯ В КАМЕРІ ЗГОРЯННЯ ГАЗОТУРБІННОГО ДВИГУНА ТА ЇЇ ВПЛИВУ НА ЕМІСІЙНІ ХАРАКТЕРИСТИКИ

Проведено дослідження впливу геометрії та розташування різних вікон підведення повітря (вторинних, розведення) на загальні температурні характеристики і формування викидів NOx в жаровій трубі трубчасто-кільцевої камери згоряння для 8 різних випадків за допомогою методів обчислювальної гідродинаміки. Моделювання виконувалося за допомогою ANSYS CFX з використанням ламінарної flamelet моделі для дослідження згоряння метано-повітряної суміші без попереднього змішання. Проведено аналіз утворення теплових і швидких NOx для прогнозування емісійних характеристик з використанням k-ε моделі турбулентності.

Ключові слова: вікон підведення повітря, емісія, горіння ,CFD, оксид азота, камера згоряння

УДК 629-735

Д.А Долматов, канд. техн. наук, доцент
Масуд Хадживанд, Аспирант
Национальный аэрокосмический университет им. Н. Е. Жуковского «Харьковский авиационный институт»

RANS МОДЕЛИРОВАНИЕ ГЕОМЕТРИИ ОКОН ПОДВОДА ВОЗДУХА В КАМЕРЕ СГОРАНИЯ ГАЗОТУРБИННОГО ДВИГАТЕЛЯ И ЕЕ ВЛИЯНИЯ НА ЭМИССИОННЫЕ ХАРАКТЕРИСТИКИ

Проведено исследование влияния геометрии и расположения различных окон подвода воздуха (вторичных, разбавления) на общие температурные характеристики и формирование выбросов NOx в жаровой трубе трубчато-кольцевой камеры сгорания для 8 различных случаев с помощью методов вычислительной гидродинамики. Моделирование выполнялось с помощью ANSYS CFX с использованием ламинарной flamelet модели для исследования сгорания метано-воздушной смеси без предварительного смешения. Проведен анализ образования тепловых и быстрых NOx для прогнозирования эмиссионных характеристик с использованием k-ємодели турбулентности.

Ключевые слова: окон подвода воздуха, эмиссия, горения, CFD, оксид азота, камера сгорания

Надійшла 05.10.2015
Received 05.10.2015

УДК 621.311.24

Качан Ю.Г., Коваленко В.Л., Лапікова О.І.
Запорізька державна інженерна академія

АНАЛІЗ ЕФЕКТИВНОСТІ ТА ПЕРСПЕКТИВ РОЗВИТКУ БІОГАЗОВОЇ ЕНЕРГЕТИКИ

Аннотація. *Біогазова енергетика має велику перспективу запровадження в Україні, але її розвиток значно гальмується через високі витрати енергії на інтенсифікацію метаногенезу (перемішування та підтримання температурного режиму в метантенку). Для підвищення ефективності виробництва біогазу необхідно розробити нові методи його інтенсифікації. Вплив електричних та магнітних полів на біомасу є недостатньо вивченим, але дослідження, проведені на різних групах мікроорганізмів, вказують на те, що при правильно підібраних параметрах він може спричинити значне збільшення обсягів продукованого біогазу і дозволити повністю або частково відмовитися від підігріву та перемішування. Це значно підвищить ефективність біогазових установок та енергетичну незалежність окремих господарств і держави в цілому. Але ці дослідження є неструктурованими і вибірковими та потребують подальшого узагальнення і уточнення, бажано, експериментально підтвердженого.*

Ключові слова: Біогаз, біометаногенез, біореактор, метаноутворюючі бактерії, електромагнітне поле, ефективність.

Зростаючий дефіцит паливних ресурсів висуває на перший план гостру необхідність пошуку альтернативних джерел енергії, бажано, відновлюваних, до яких належить біогаз — суміш з 65% метану, 30% вуглекислого газу, 1% сірководню і незначних домішок азоту, кисню, водню і чадного газу [1]. В 1 м^3 біогазу міститься енергія, еквівалентна 0,6 м^3 природного газу, або 0,74 і 0,66 літри нафти чи дизельного палива, відповідно. Тобто, маючи достатню кількість згаданого енергоносія, можна значно зменшити залежність країни від імпортних енергоносіїв.

Як правило, при виробництві метану значна кількість отриманої енергії витрачається на забезпечення процесу бродіння, а саме: дотримання необхідного температурного режиму всередині біореактору та перемішування субстрату, без яких ефективність процессу значно зменшується. Крім того, вона залежить як від обраної технології, матеріалів і конструкції основних їх елементів, так і від кліматичних умов у районах їх розташування. Середнє споживання виробленої енергії для забезпечення процесу в самому біореакторі у широтах України становить: теплової — 15-30%, й, додатково, електричної — 6-9 % [2]. При цьому після очищення біогазу від негорючих і шкідливих домішок його собівартість наближається до вартості природного, що може бути економічно недоцільним.

Відомо, що утворення біогазу відбувається при температурах від 0°С до 97°С і у цьому проміжку виділяють, умовно, три температурні режими [2]: психрофільний (до 20-25°С), мезофільний (25-40°С) і термофільний (понад 40°С). Перший спостерігається в установках без підігріву, в яких відсутній контроль